8-2019

# Immobilization of Electrocatalytically Active Gold Nanoparticles on Nitrogen-Doped Carbon Fiber Electrodes

Daniel Mawudoku
*East Tennessee State University*

# Immobilization of Electrocatalytically Active Gold Nanoparticles on Nitrogen-Doped Carbon Fiber Electrodes

A thesis

presented to

the faculty of the Department of Chemistry

East Tennessee State University

In partial fulfillment

of the requirements for the degree

Master of Science in Chemistry

by

Daniel Kwasi Mawudoku

August 2019

Dr. Gregory W. Bishop, Chair

Dr. Dane W. Scott

Dr. Hua Mei

Keywords: Gold nanoparticles, methanol oxidation, electrocatalysis, nitrogen-doped carbon fiber ultramicroelectrode, soft nitriding

ABSTRACT

Immobilization of Electrocatalytically Active Gold Nanoparticles on Nitrogen-Doped Carbon Fiber Electrodes

by

Daniel Kwasi Mawudoku

Studies of single, isolated nanoparticles provide better understanding of the structure-function relationship of nanoparticles since they avoid complications like interparticle distance and nanoparticle loading that are typically associated with collections of nanoparticles distributed on electrode supports. However, interpretation of results obtained from single nanoparticle immobilization studies can be difficult to interpret since the underlying nanoelectrode platform can contribute to the measured current, or the immobilization technique can adversely affect electron transfer. Here, we immobilized ligand-free gold nanoparticles on relatively electrocatalytically inert nitrogen-doped carbon ultramicroelectrodes that were prepared via a soft nitriding method. Sizes of the particles were estimated by a recently reported electrochemical method and were found to vary linearly with deposition time. The particles also exhibited electrocatalytic activity toward methanol oxidation. This immobilization strategy shows promise and may be translated to smaller nanoelectrodes in order to study electrocatalytic properties of single nanoparticles.

# DEDICATION

This research work is dedicated to the Almighty God and to my mother Regina Yawa Torgbe, for the support that you have always been in my life.

# ACKNOWLEDGMENTS

My first and foremost thanks go to the Almighty God who has been my shield and protection all my life. He has made it all possible and fruitful. Secondly, I say a big "thank you" to Dr. Bishop, Gregory W. for accepting me to be a part of your research group. The beginning was not easy for me, but you never relented in your patience, support and encouragement for me. You were always there (even in the oddest of times) to provide advice, guidance and direction whenever I called upon you. I owe you a debt of gratitude. May God Almighty continue to guide and protect you.

Thirdly, I want to thank Dr. Scott, Dane W. and Dr. Mei, Hua (my thesis committee members); I am highly honored to have you on my committee. Your pieces of advice, suggestions and corrections have been invaluable. Thank you so much. May God Almighty protect and keep you safe always. My appreciation also goes to all faculty and staff of the chemistry department especially Dr. Roginskaya, Marina and Dr. Mohseni, Ray for their support and assistance throughout my stay in the department. To you Enoch Amoah, Chidiebere Ogbu, Elisha Adeniji, Haley Davis, Caitlin Millsaps, Fayez Alharbi, George Affadu-Danful and Theophilus Neequaye, thank you so much for all the assistance you provided me in the lab. You have all been great lab mates.

Finally, I will like to thank the American Chemical Society Petroleum Research Fund (Award # 58123 — UN15) for providing financial support for this research work.

TABLE OF CONTENTS

LIST OF TABLES

Table Page

LIST OF FIGURES

LIST OF ABBREVIATIONS

| | |
|---|---|
| Au-N-CF-UME | Gold-modified nitrogen-doped carbon fiber ultramicroelectrodes |
| AuNP | Gold nanoparticle |
| Avg | Average |
| CF-UME | unmodified carbon fiber ultramicroelectrode |
| CV | Cyclic voltammetry |
| FcMeOH | Ferrocene methanol |
| HER | Hydrogen evolution reaction |
| ID | Internal diameter |
| LSV | Linear sweep voltammetry |
| MeOH | Methanol |
| MNP | Metal nanoparticle |
| N-CF-UME | Nitrogen-doped carbon fiber ultramicroelectrode |
| NP | Nanoparticle |
| NS | Nanosphere |
| OD | Outer diameter |
| ORR | Oxygen reduction reaction |
| SA | Surface area |
| SCE | Saturated calomel electrode |
| SNP | Single nanoparticle |
| SNPE | Single nanoparticle electrode |
| UME | Ultramicroelectrode |
| XPS | X-ray Photoelectron Spectroscopy |

# CHAPTER 1

# INTRODUCTION

## Metal Nanoparticles and Electrocatalyst?

Nanoparticles (NPs) are particulate materials with sizes in the range of 1-100 nm.[1] Compared to their bulk counterparts, NPs possess high surface-area-to-volume ratios and advantageous physical and chemical properties. Due to these attributes, NPs have been widely studied[2,3] and applied in catalysis, medicine, sensing, imaging, and energy. Metal nanoparticles (MNPs) have been the subject of much research for more than two decades due to their unique thermal, optical and electrical properties as well as their abilities to act as catalysts and electrocatalysts for important processes like those involved in fuel cells (e.g. direct methanol fuel cell) and sensing (e.g. dopamine detection).[4,5]

For example, many research efforts have been directed at methanol oxidation using MNP electrocatalysts for the direct methanol fuel cells.[6] Methanol oxidation is a very important reaction and complete oxidation of methanol proceeds via a six-electron process (equation 1) involving CO or HCHO and HCOOH as intermediates (equation 2).[7]

$$CH_3OH + H_2O \rightarrow CO_2 + 6H^+ + 6e^- \quad (1)$$

$$CH_3OH \rightarrow (CO, HCOH, HCOOH) \begin{cases} \rightarrow CO_{ad} \rightarrow CO_2 \\ \rightarrow (HCOH, HCOOH) \rightarrow CO_2 \end{cases} \quad (2)$$

Although the thermodynamic potential for methanol oxidation (0.02 V) is about the same as the equilibrium potential for hydrogen oxidation, the rate of methanol oxidation is much slower (several orders of magnitude slower), hence the need for a catalyst.[7,8] The most active and widely used MNP electrocatalyst for methanol oxidation reaction has been platinum. Huang et al. examined the electrocatalytic ability of platinum nanoparticles (PtNPs) supported on activated

carbon fiber and carbon black toward methanol oxidation in acidic medium. PtNPs supported on activated carbon fiber were found to exhibit narrower size range (1.5 to 3.5 nm) and smaller average size (2.4 nm) compared to those on carbon black (1.0 to 9.0 nm and 2.9 nm, respectively). Compared to PtNPs on carbon black, PtNPs on activated carbon fiber also showed 2.4 times higher electrocatalytic activity towards methanol oxidation, which was attributed to more uniform dispersion, lower agglomeration, and smaller size.[9] However, high cost of platinum and its high susceptibility to poisoning by intermediates of methanol oxidation reaction (such as CO) have necessitated the search for a suitable alternative catalyst to platinum.[10,11]

Gold is gaining acceptance as a good catalyst for the oxidation of methanol due to some important qualities it possesses. First, though gold is not as catalytic as platinum for methanol oxidation, it is also reportedly not susceptible to CO poisoning.[6,12] Electrocatalytic activity of gold toward methanol oxidation is also reportedly higher in alkaline medium than in acidic medium.[6,11] Zhang investigated the electrocatalytic activity of gold nanoparticles (AuNPs) supported on activated carbon toward methanol oxidation in an alkaline medium using cyclic voltammetry. Zhang's results showed that the AuNPs (average diameter 6 nm) exhibit high electrocatalytic activity toward the methanol oxidation reaction, with the onset of the oxidation reaction at -100 mV vs. the saturated calomel electrode (SCE) and peak anodic current density obtained at +360 mV (vs. SCE).[13]

## Effects of Nanoparticle Structure on Electrocatalytic Behavior

Numerous studies have shown that the electrocatalytic properties of MNPs depend on their size[4], geometry[14], crystallite structure[6] and surface attached ligands[15]. For example, Shao et al. examined the effect of PtNP size on its catalytic activity toward oxygen reduction reaction (ORR) in acidic medium (equation 3).

$$O_2\,(g) + 4\,H^+(aq) + 4\,e^- \longrightarrow 2\,H_2O(l) \qquad (3)$$

Their results demonstrated that the mass activity (electrocatalytic current in mA per mass of Pt in mg) of PtNPs for the ORR increased by 2-fold as the particle size increased from 1.3 to 2.2 nm but decreased upon further increase in particle size to 5 nm.[16] In another study, Bansal et al. observed shape-dependent electrocatalytic behavior of silver NPs with higher catalytic activity exhibited at nanoprism shapes than at nanocubes and nanosphere shapes toward hydrazine oxidation, formaldehyde oxidation and hydrogen peroxide reduction reactions.[14]

While numerous studies[4,5,8,9,13-16,26] have been undertaken in a bid to understand the relationship between structural properties and electrocatalytic activity of MNP electrocatalysts, most of these works have employed large numbers (collections) of MNPs[17-20] dispersed on conductive solid supports (usually carbon) and as such, only provide an average representation of the MNP structure-activity relationship. Electrocatalytic measurements obtained from such systems can be very difficult or impossible to interpret due to the presence of unavoidable and difficult-to-quantify interfering factors related to the spatial distribution, such as interparticle distance and particle loading, and heterogeneity, such as variations in particle shape and size.[20,21]

In the pursuit of a better understanding of the relationship between nanoparticle structure and electrocatalytic behavior, methods including NP impact (or collision) on an ultramicroelectrode (UME) surface[22-27] as well as the immobilization of a single NP on a nanometer size electrode[14-16,28] have recently emerged for studying individual, isolated MNPs. These types of single NP (SNP) electrochemical techniques provide measurements of electrocatalytic properties that are unobscured by spatial and ensemble averaging effects.

The impact method involves immersing an UME into an electrolyte (containing freely diffusing, catalytic NPs) and holding it at such a potential that, no electrochemical reaction is

observed in the absence of the NPs. However, as soon as a NP collides (impacts) with the UME surface, electrochemical response (in the form of transient "blips"[22], "spikes"[23], or "step-like"[24] changes in the current-time response) are observed. The magnitude of current-time responses is known to be related to NP size, while the frequency (number of responses in given time) of these transient signals are related to concentration. While NP impact measurements have been carried out for various electrocatalytic systems, these experiments[22-26] often involve cumbersome data collection and processing steps. Fast current-time measurements are required, and analysis involves identifying small signals in the presence of considerable electrical noise. By comparison, a smaller number of published reports has involved immobilization for electrochemical measurement of single nanoparticles, but this method can simplify the study of SNPs by enabling the use of electrochemical methods like voltammetry.[14,15,28]

## Electrochemical Measurements of Nanoparticles by Single-Nanoparticle Immobilization

In the single-nanoparticle immobilization method, an individual, isolated NP is attached to the surface of an electrode. While deposition of NPs on larger electrodes (UMEs and macroelectrodes) typically results in immobilization of NP ensembles, reducing electrode size to the nanometer level (nanoelectrode) is necessary to isolate a single NP on the electrode surface.[15,28-30] To successfully immobilize only one NP on a nanoelectrode, it is important that the size of the electrode is similar to or smaller than the nanoparticle of interest in order to reduce the chance of attaching more than one particle to the electrode surface.[15,28,31-33] Fabrication of nanoelectrodes is therefore a crucial step in successful application of SNP immobilization.

### Fabrication of Nanoelectrodes

Nanoelectrodes can be prepared with various geometries including conical[34,35], nanopore[36], spherical cap[37] and disk (recessed[38] and inlaid[39]) electrodes. Fabrication of

nanoelectrodes can be accomplished using techniques such as chemical vapor deposition (of metals and non-metals) and laser-assisted micropipette pulling. Laser-assisted micropipette pulling is a widely used method for the preparation of disk-shaped nanoelectrodes.[30-32,36,38,40] Here, a micrometer-sized strand of a conductive electrode material (metal wire or carbon fiber) is inserted or aspirated into a glass capillary tube (borosilicate or quartz), which is then clamped on each end between two pulleys. With the help of heat from a laser applied to the middle of the capillary tube, the glass capillary is drawn into two pipettes by the pulleys.

Depending on the pulling parameters (Heat, Pull, etc.), the electrode material may be sealed inside each pipette or may need to be sealed by additional post-processing steps involving thermal annealing[32] or epoxy[40]. Since the sealed end of the electrode material is usually completely encased in the glass after pulling or post-process treatment, it is often necessary to expose the electrode via beveling or manual polishing. Varying the pulling and polishing parameters allows one to control the size and shape of the electrodes.[30,38,39,41-43] Although Shao et al. were the first to demonstrate the fabrication of silver and platinum nanoelectrodes using the laser-assisted micropipette pulling method[39], several other research groups subsequently used this technique to fabricate nanoelectrodes of gold[32], platinum[30,38] , silver[42] and carbon[15,34] for various electrochemical studies.

Immobilization Strategies

Immobilization of single MNPs on nanoelectrodes can be accomplished through several means including direct adsorption, electrostatic interaction, electrodeposition and covalent binding (Table 1).[15,28,30,44] To probe the electrochemical properties (e.g. electrocatalytic activities) and understand how variations in NP size affect electrocatalytic properties, Zhang and co-workers attached a single AuNP (ranging in size from 15 nm to 30 nm) to a platinum

nanoelectrode (10 nm) that was modified with an aminated silane or thiol linker.[30] Immersing the modified Pt electrode in a solution of citrate-capped AuNPs enabled the electrostatic adsorption of a single AuNP onto the Pt electrode, thus forming a single nanoparticle electrode (SNPE). Techniques such as cyclic voltammetry, transmission electron microscopy and underpotential deposition of copper were used to thoroughly confirm the presence of the immobilized AuNP.

Compared to the bare Pt nanoelectrode in 5.0 mM $K_3Fe(CN)_6$ solution (containing 0.2 M KCl), there was an increase in state steady limiting current associated with the Au SNPE, demonstrating improved electron transfer between the electrode and the redox molecule. Furthermore, the electrodes (both bare Pt electrode and Au SNPE) were used to probe catalytic activity toward ORR in an alkaline (KOH) medium. Their results showed that the half-wave potential ($E_{1/2}$) for the ORR at the Au SNPE shifted to less negative (-130 mV, -75 mV and -35 mV respectively for 14 nm, 18 nm and 24 nm Au SNPEs) than that for the bare Pt electrode (-365 mV). This clearly indicated that the Au SNPE exhibited enhanced electrocatalytic activity compared to Pt, and that the catalytic activity of the Au SNPE varied with the size of the AuNPs.[30,33]

In another study, Sun el ta. investigated the electrochemical behavior of single AuNPs immobilized on Pt nanoelectrodes by electrodeposition. The presence of the single gold NP was verified using cyclic voltammetry. Results from this study showed that the potential of the gold oxide peak or the gold oxide reduction peak was dependent on size.[44]

**Table 1:** Summary of selected studies based on the immobilization technique.

| Electrode Type, Radius (nm) | NP type, Radius (nm) | Immobilization Technique | Reaction | Reference |
|---|---|---|---|---|
| Carbon (3) | Au (5) | Direct and electrostatic adsorption, covalent binding | HER | 15 |
| Carbon (~50) | Pt (150) | Electrodeposition | ORR | 28 |
| Pt (10) | Au (15) | Electrostatic adsorption | ORR | 30 |
| Pt (8.9) | Au (42) | Electrodeposition | Au oxide reduction | 44 |

ORR and HER are abbreviations for oxygen reduction reaction and hydrogen evolution reaction respectively.

While deposition of single AuNPs on Pt electrodes has been demonstrated, complications can arise from employing metal nanoelectrodes as platforms for studying metal nanoparticles. For example, both AuNPs and the Pt nanoelectrodes act electrocatalytically toward the ORR, which can make it difficult to determine the extent to which each (the AuNP and the Pt electrode) contributes to the overall current observed.[15] To circumvent this complication, Mirkin's group[15] immobilized single AuNPs on carbon nanoelectrodes. Besides having good electrical conductivity, the carbon support was relatively catalytically inert to the hydrogen evolution reaction (HER) they were studying (equation 4). Thus, electrocatalytic behavior observed could be attributed solely to the immobilized AuNP.[15]

$$2\ H^{+}\ (aq) + 2\ e^{-} \rightarrow H_2\ (g) \qquad (4)$$

Three different immobilization strategies (direct adsorption, electrostatic interaction and covalent binding) were employed to attach citrate-capped AuNPs to carbon electrode supports. The carbon electrode was simply immersed in a solution of negatively charged citrate-capped AuNPs in order to immobilize a single AuNP by direct adsorption. Electrostatic adsorption of

single AuNPs on the carbon electrode was achieved by modifying the carbon surface with a positively charged, electrodeposited polyphenylene layer. In separate experiments, the terminal amines on the polyphenylene molecules were also converted into diazonium groups followed by reducing them electrochemically so that they formed strong carbon-gold covalent bonds with the AuNPs.[15]

Mirkin and co-workers then compared the electrocatalytic response toward HER at both bare carbon and polyphenylene-modified carbon electrodes (each with AuNPs attached). They observed that the onset potential for the HER at the AuNP directly adsorbed onto the bare carbon electrode shifted to a more positive value (more than 500 mV) than that at the AuNPs electrostatically adsorbed or covalently bound to polyphenylene-modified electrodes. This indicated that the AuNP immobilized by direct adsorption on the bare carbon electrode was more electrocatalytically active than those immobilized on the polymer-modified electrodes. According to Mirkin and co-workers, this observed difference in electrocatalytic activity could be due to the insulating capabilities of the polyphenylene film, which impeded electron transfer between the carbon surface and the immobilized AuNP.[15] Although the inert carbon served as a suitable support for probing the HER, challenges brought on by the insulating polyphenylene film and the surface active-site blocking capping agents on the AuNPs suggest alternative strategies for immobilizing single metal nanoparticles on carbon electrodes are worth pursuing. Nitrogen-doped carbon materials may be a suitable strategy to address the above-mentioned challenges.

## Soft Nitriding of Carbon Materials for Immobilizing Metal Nanoparticles

Doping of carbon materials with nitrogen can be done either directly during synthesis or via post-treatment of the carbon material.[45] Recently, Liu et al. reported that highly

electrocatalytic, ligand-free noble metal nanoparticles can be immobilized on various carbon supports (including mesoporous carbon, carbon black and activated carbon) by doping the carbon materials with nitrogen through a process called soft nitriding.[46]

Soft nitriding involves low-temperature annealing ($\leq 300\ ^{o}C$) of a carbon support with urea. Heating reportedly decomposes urea into ammonia and isocyanic acid (equation 5).

$$(CO(NH_2)_2 \rightarrow NH_3 + HOCN) \qquad (5)$$

Isocyanic acid forms ureido groups through addition reactions with carboxylic and hydroxyl groups on the surface of the activated carbon material. Integration of nitrogen species into the graphitic layer of the carbon was carried out by ammonia.[46] While there were no detectable nitrogen species on the Printex G carbon prior to nitriding, X-ray Photoelectron Spectroscopy (XPS) data showed that 19% of the total surface atom composition of the Printex G carbon after soft nitriding was nitrogen.[46] In previous work from our research group, Affadu-Danful found that nitrogen-doped carbon fiber UMEs could also be prepared by the soft nitriding method. [47] XPS results indicated that soft nitriding of carbon fiber using urea resulted in a 3.5 fold increase in surface nitrogen content (from 4.08 to 13.94%).[47]

Both ureido groups and the nitrogen-doped graphitic species reportedly induce a strong affinity of the carbon surface for metal precursor ions (e.g., $AuCl_4^-$) which enables deposition of ultra-small MNPs. MNP nucleation and growth occurs directly on the nitrided carbon at the nitrogen containing sites upon addition of sodium borohydride reducing agent (equation 6)[48].

$$8\ HAuCl_4 \cdot 3H_2O + 3\ NaBH_4 \rightarrow 8\ Au + 3\ NaB(OH)_4 + 12\ H_2O + 32\ HCl \qquad (6)$$

The nitrogen moieties on the carbon support also reportedly stabilize the MNPs and thus prevents overgrowth. The strategy proved to be a versatile one for depositing highly active sub-2 nm metal nanoclusters of various metals, including gold, platinum, and palladium on carbon

black, mesoporous carbons, and activated carbons.[46] In our group, Affadu-Danful found that gold NPs could similarly be deposited preferentially on nitrogen-doped carbon fiber UMEs compared with unmodified carbon fiber UMEs.[47] Cyclic voltammograms (CV) of nitrogen-doped carbon fiber UMEs showed both gold oxide formation and gold oxide reduction peaks after deposition of gold, while no CV signals associated with gold were observed using unmodified carbon fiber UMEs even after 24 hours of attempted deposition.[47] Though the presence of gold was confirmed, AuNPs were not characterized in terms of size or electrocatalytic behavior.

## Research Goals

Electrochemical and electrocatalytic studies of metal NPs immobilized on solid electrode supports are faced with many challenges such as, the ligands used to stabilize and prevent aggregation and overgrowth of NPs during synthesis generally block active sites on NPs.[15,27] In addition, electrocatalytic responses observed at some solid electrode supports (e.g., Pt) make analysis of electrochemical signals from immobilized NPs difficult.[30,33] Also, linker molecules used to connect NPs onto solid supports sometimes interfere with electron transfer between the underlying electrode support and the immobilized NP. The ability to synthesize metal NPs in the absence of ligands and immobilize them on electrocatalytically inert substrates is highly desirable, particularly in the study of NPs at the single NP level.

In this study, we immobilized electrocatalytically active gold nanoparticles on nitrogen-doped carbon fiber ultramicroelectrodes (UMEs) to determine the potential applicability of this method for electrochemical and electrocatalytic measurements at the single NP level. We accomplished AuNP immobilization by adapting a recently reported method[46] for synthesizing and directly immobilizing metal NPs onto catalytically inert carbon supports. This technique does not involve the use of stabilizing ligands (capping agents) during the synthesis of the metal

NPs nor does it use linker molecules in the immobilization of the NPs onto the solid support. Thus, we should be able to study these NPs without the complicating factors that stabilizing ligands and catalytically active solid supports bring to the analysis (that is blockage of active sites on NPs and contributing to the observed electrochemical response, respectively). Furthermore, we should be able to compare electrocatalytic activities at both capped and uncapped NPs. With a previous report from our group clearly demonstrating that gold nanoparticles can be immobilized on nitrided carbon fiber, the specific aims for the work presented here are to characterize and optimize the AuNPs deposited on the nitrided carbon fiber electrodes, determine their sizes, and evaluate their catalytic activities toward the methanol oxidation reaction.

# CHAPTER 2

# EXPERIMENTAL

## Materials

Potassium chloride (99+%), urea (99+%) and sulfuric acid (95-98%) were purchased from Sigma-Aldrich, while hydrochloric acid (35-37%), sodium hydroxide and nitric acid (68-70%) were obtained from VWR Analytical. Potassium perchlorate (99+%) and tetrachloroaurate (III) trihydrate were from Alfa Aesar. Sodium borohydride and methanol (99.9%) were from Fischer Scientific. Ferrocene methanol (≥97%), potassium bromide (99.5%) and perchloric acid (70%) were from Acros Organics, Allied Chemical and Fluka Analytical, respectively. Borosilicate glass capillaries with filament (O.D 1.0 mm, I.D 0.50 mm and I.D. 0.58 mm) were from Sutter Instrument Co. (Novato, CA). Silver conductive adhesive paste was from Beantown Chemical (Hudson, NH). Nichrome wire was obtained from Parr Instrument Co. (Moline, IL) and carbon fiber (7 μm in diameter) was bought from Goodfellow Cambridge Limited (Huntington, England). Nitrogen gas was obtained from Airgas. Ultrapure water (18.2 MΩcm) was used to prepare all aqueous solutions used in this study. All chemicals for this study were used as received without any further purification.

## Nitrogen Doping of Carbon Fiber

Previous work from our group[47] demonstrated that nitrogen doping by the method reported by Liu et al.[46] is also applicable to carbon fiber. XPS results revealed that nitriding increased the surface nitrogen content of the carbon fiber by about four times what was originally present.[47] Nitrogen doping of the carbon fiber was carried out in similar manner as previously reported by our group.[47] Briefly, 0.28 g carbon fiber was mixed with 0.42 g urea. The

mixture was then heated at 150 $^{o}$C for 2 hours in an oven. This was followed by further heating at 250 $^{o}$C for another 2 hours. The as-prepared nitrogen-doped carbon fiber was then carefully washed with water, followed by ethanol. After drying the washed carbon fiber in the oven at 60$^{o}$C for 6 hours, the fiber was ready to be used.[46]

## Fabrication of Carbon Fiber Ultramicroelectrode (CFUME)

To fabricate the CFUMEs, a single strand (7 μm) of either nitrogen-doped (N-CF) or unmodified carbon fiber (CF) was aspirated into a borosilicate capillary tube by vacuum. The capillary tube containing the carbon fiber (Figure 1) was then pulled into two halves (with the carbon fiber sealed in each) with the help of Sutter P-2000 laser pipette puller using a two-line program with the following pulling parameters:

First line: Heat = 400, Filament = 0, Velocity = 30, Delay = 220, Pull = 0

Second line: Heat = 450, Filament = 1, Velocity = 20, Delay = 180, Pull = 0

The pulling parameters (such as heat, velocity, delay etc.) are dimensionless quantities and by no means indicate the actual temperature, velocity or time for the pull. A piece of nichrome or stainless steel wire was painted with silver adhesive conductive paste and then inserted through the open end of the pulled capillary to establish an electrical connection with the carbon fiber for electrochemical experiments. Epoxy was then applied to the open end of the tube to secure and ensure the wire was always in contact with the fiber.

To expose the carbon fiber sealed in the capillary tube, the tip of the sealed end of the capillary tube was first manually polished on an 800-grit sand paper. Further polishing was done on 1000-grit and 2000-grit sand papers. As polishing continued and the electrochemical signal from the electrode approached sigmoidal shape, the grit paper was switched to a finer grit size

(1000 and then 2000) to complete the polishing. For every minute of polishing, the electrode was scanned in 0.5 mM ferrocene methanol (FcMeOH) solution (containing 0.1 M KCl) versus Ag/AgCl reference electrode to test for the electrochemical signal of the exposed carbon fiber. The polishing was continued until the electrode produced a sigmoidal shaped cyclic voltammogram (Figure 2).[41-43]

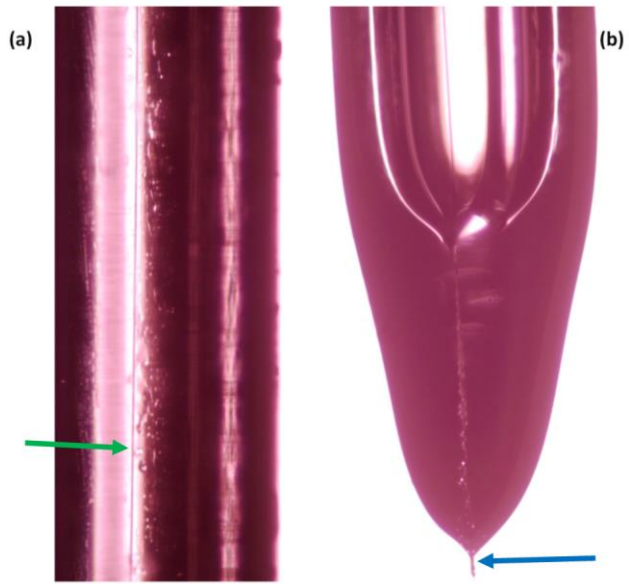


**Figure 1:** Images of carbon fiber (CF) in borosilicate capillary tube. CF before (a) and after (b) pulling to fabricate a CF electrode. Green arrow points to the carbon fiber in the tube before pulling. Blue arrow points to the tip of the pulled tube showing glass encased fiber pointing out.

Electrochemical Characterization of Carbon Fiber Ultramicroelectrodes (CFUMEs)

Cyclic voltammetry was used to estimate the sizes of both nitrogen-doped carbon fiber electrodes (N-CF-UMEs) and unmodified carbon fiber ultramicroelectrodes (CF-UMEs). All electrochemical measurements in this study were done using Bioanalytical Systems Epsilon electrochemical workstation. A two-electrode system was employed, with the carbon fiber electrode serving as the working electrode versus Ag/AgCl (1 M KCl) reference electrode. The potential of the working electrode was scanned (swept) from 0 mV to 400 mV and back to 0 mV in 5 mL of 0.5 mM FcMeOH solution containing 0.1 M KCl as supporting electrolyte.

Ultramicroelectrodes give well-known sigmoidal-shaped voltammograms for common redox probes like FcMeOH with steady state current (Iss) of the electrode reaction proportional to the radius of the electrode as given in equation 1 below[15,30]. From equation 7, the radius of the electrode can be estimated.

$$Iss = 4nFDrC \qquad (7)$$

Where n is the number of electrons transferred per mole of reactant (redox molecule), F is Faraday's constant (96485 C/mol), D and C are the diffusion coefficient ($7.8 \times 10^{-6}$ $cm^2/s$ for FcMeOH15) and the bulk concentration (in $mol/cm^3$) of the redox molecule, respectively, and r is the radius of the electrode (in cm). The scan rate for all electrochemical measurements made for characterizing electrodes was 25 mV/s based on previous report.[47] For this study, only electrodes showing sigmoidal-shaped cyclic voltammograms (Figure 2) were used as electrode supports for immobilization of the AuNPs. Based on equation 1, the average radii for CF-UMEs and N-CF-UMEs used in all subsequent studies here were 4.52±0.82 µm and 1.62±0.41 µm, respectively.

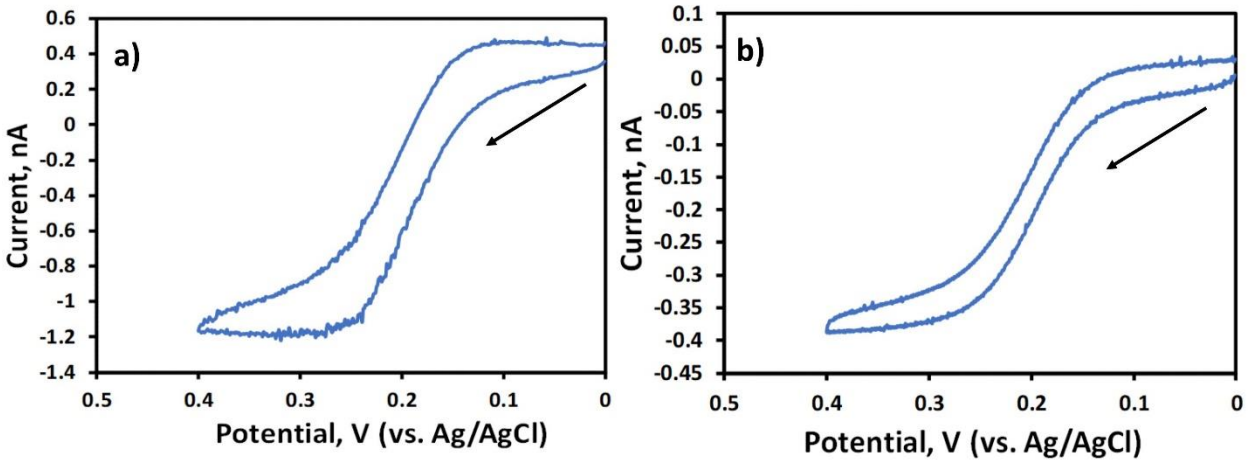


**Figure 2**: Representative cyclic voltammograms showing the electrochemical response of CF-UME and N-CE-UME in 0.5mM FcMeOH containing 0.1M KCl used for estimating electrode size. The scan rate 25 mV/s.

## Immobilization of AuNPs on CF-UMEs and N-CF-UMEs

Deposition of AuNPs onto CF-UMEs and N-CF-UMEs was attempted by chemical reduction of $HAuCl_4$ using $NaBH_4$ as the reducing agent.[46] First, the tip of the CF-UME or N-CF-UMEs was immersed in a 10 mL beaker containing 5 mL of 0.1 mM gold solution ($HAuCl_4 \cdot 3H_2O$). While stirring on a magnetic stirrer, 30 µL of a freshly prepared 0.1 M $NaBH_4$ was added and the stirring continued for varying amounts of time (10 seconds, 10, 30, 60 minutes and 12 hours). Upon addition of $NaBH_4$, the color of the gold solution turned from yellow to wine red, indicating the formation of AuNPs. At the end of a designated deposition time, the electrode was taken out of the AuNP solution and rinsed with water.

## Nanoparticle Size Determination by Electrochemical Surface Area-to-Volume Ratio

In order to characterize AuNPs deposited on CF-UMEs and N-CF-UMEs, an electrochemical method that reported by Sharma et al.[49] was employed. This technique for sizing spherical AuNPs is based on measuring electrochemical signals that are proportional to surface area (SA) and volume (V) of NPs immobilized on the electrode surface. SA is proportional to the charge associated with the reduction of a surface oxide layer that can be formed on AuNPs by scanning the working electrode to oxidizing potentials in 0.1 M $HClO_4$. The gold oxide reduction peak potential ($E_p$) in the $HClO_4$ occurs in the range of 1000 mV to 600 mV vs. Ag/AgCl[50-52] during a subsequent scan of the electrode towards negative potentials. Integration of the gold oxide reduction peak obtained from cyclic voltammetry yields the charge required to completely remove the surface oxide layer. Reduction of a monolayer of gold oxide produces about 400 µC/cm$^2$.[52] Therefore, the charge associated with reduction (removal) of the gold oxide layer is proportional to the SA and total number of the AuNPs.

Particle volume can similarly be determined by electrochemical measurements as AuNPs can undergo oxidative dissolution in aqueous bromide solution to form tetrabromoaurate, $AuBr_4^-$. The charge that corresponds to this process can be obtained using linear sweep voltammetry (LSV).[49,53-55] The position of $E_p$ for oxidative dissolution has been shown to range from 734 mV to 913 mV vs. Ag/AgCl depending on the size and extent of aggregation of the AuNPs with larger and aggregated particles exhibiting more positive $E_p$ values.[55]

Assuming a spherical shape for immobilized, monodisperse AuNPs, electrochemical signals proportional to SA and V can be used to determine particle radius, r, since the surface area-to-volume ratio (SA/V), is equivalent to the quantity 3/r:

$$\frac{SA}{V} = \frac{3}{r} \qquad (8)$$

Using this method, Sharma et al. determined the sizes of citrate-capped gold nanospheres (NSs) electrostatically adsorbed onto glass/ITO electrodes functionalized with APTES (3-aminopropyltriethylsilane). The NSs ranged in diameter from 4 nm to 70 nm. Results from their study showed good agreement with values obtained using electron microscopy.[49]

To determine the size of AuNPs deposited on a N-CF-UME or CF-UME by electrochemical SA/V measurements, the UME was first placed in 0.1 M $HClO_4$ and scanned from -200 mV to 1400 mV and back to -200 mV vs. Ag/AgCl using cyclic voltammetry to acquire the charge associated with the gold oxide reduction peak. This charge is proportional to the surface area of the AuNP. The same electrode was then immersed in 0.01 M KBr solution containing 0.1 M $KClO_4$ and scanned from -100 mV to 1200 mV using LSV to obtain the $AuBr_4^-$ peak for determining the volume of AuNPs. Integration of the $AuBr_4^-$ peak provided the total volume of AuNP.

## Methanol Oxidation Reaction

To examine catalytic activity towards the methanol oxidation reaction under alkaline conditions, potentials of CF-UMEs, N-CF-UMEs, and gold modified nitrogen-doped carbon fiber ultramicroelectrodes (Au-N-CF-UMEs) were scanned from -600 mV to +600 mV and back to -600 mV vs. the saturated calomel electrode (SCE) in 5 mL of deoxygenated 0.1 M NaOH solution in the absence and presence of 1.0 M methanol at a scan rate of 25 mV/s based on report.[56]

# CHAPTER 3

# RESULTS AND DISCUSSION

## Immobilization of Ligand-Free AuNPs on CF-UMEs and N-CF-UMEs

After attempted deposition of AuNPs for 1 hour on both CF-UMEs and N-CF-UMEs, cyclic voltammetry (CV) was performed on the electrodes in 0.5 M $H_2SO_4$ to examine for evidence of successful immobilization of AuNPs (Figure 3). CV peaks that are consistent with the presence of Au on the electrode surface were observed only for N-CF-UMEs after deposition of AuNPs (Figure 3b). The broad peak at 1.21 V vs Ag/AgCl is consistent with the formation of gold oxide[50,51], while the peak at 0.97 V vs. Ag/AgCl corresponds to the reduction of gold oxide.[50] The electrodes were subjected to different immobilization times, and we observed that AuNPs could be deposited on the N-CF-UMEs in as little as 10 seconds (Figure 4b). However, there were no observable AuNP signals on the CF-UME until after more than 10 hours of attempted immobilization (Figure 4a).

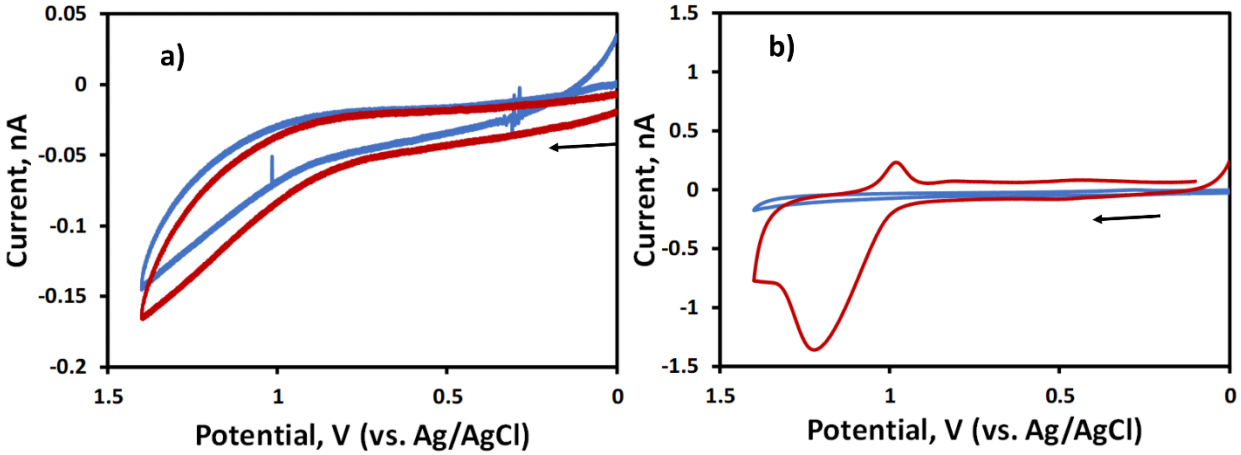


**Figure 3:** Representative CVs comparing electrochemical responses of CF-UME and N-CF-UME after 1-hour AuNP deposition in 0.5M $H_2SO_4$. CF-UME (a) in $H_2SO_4$ before (blue) and after (red) attempted AuNP deposition. N-CF-UME (b) before (blue) and after (red) AuNP deposition. The arrows indicate the direction of the forward scan. The scan rate was 25 mV/s.

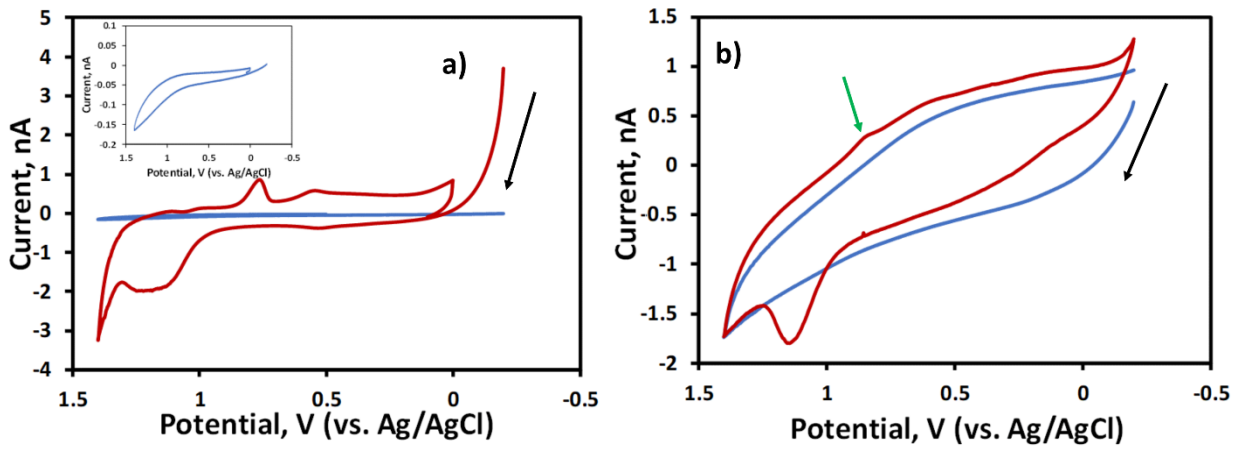


**Figure 4:** CV responses comparing least deposition time for CF-UME and N-CF-UME. CF-UME (a) and N-CF-UME (b) in 0.5 M $H_2SO_4$ before (blue) and after (red) AuNP deposition. The response in (a) was obtained after more than 10 hours of attempted immobilization while the response in (b) was obtained after 10 seconds of attempted AuNP immobilization. The black arrow shows the direction of forward scan. The green arrow points to gold oxide reduction peak. Insert in (a) is the CV response for the bare CF-UME before AuNP immobilization was attempted.

The soft nitriding process used to prepare N-CF from CF involves low-temperature annealing with urea, which introduces pyridinic and amine/amide groups on the carbon fiber surface.[46] The introduction of these nitrogen-containing moieties on the surface of carbon materials increases the affinity of the carbon surface for the anionic precursors for the noble metals (e.g. Au, Pt and Pd) and reportedly stabilize metal nanoparticles during $NaBH_4$ reduction to prevent overgrowth.[46] This leads to preferential deposition of AuNPs on N-CF-UMEs compared to CF-UMEs (Figures 3-4).[46] The presence of AuNPs on CF-UMEs after long deposition times (>10 hrs, Figure 4a) is likely due to adsorption of AuNPs grown in solution rather than direct growth of AuNPs on the carbon surface.

## Determination of Size of the Immobilized AuNPs

Sizes of AuNPs deposited on N-CF-UMEs and CF-UMEs were estimated using a previously reported electrochemical method. It is based on the determination of surface area-to-volume ratio from charges (in coulombs, C) associated with surface oxide reduction and oxidative dissolution of AuNPs[49]. To determine charge related to surface oxide reduction, potentials of Au-N-CF-UMEs were scanned in aqueous $HClO_4$. The Au oxide reduction peak (Figure 5a) was integrated to obtain the charge associated with the reduction of the surface oxide layer, which is proportional to the surface area (SA) of the AuNP. Equation 9 shows the reaction for the gold oxide reduction.[49]

$$Au_2O_3 + 6H^+ + 6e^- \rightarrow 2Au + 3H_2O \qquad (9)$$

The same electrode was then immersed in KBr solution containing $KClO_4$ and scanned using linear sweep voltammetry (LSV) in order to determine the charge associated with complete oxidative dissolution of AuNPs to $AuBr_4^-$ (Figure 5b). This charge is proportional to AuNP volume (V). Equation 10 is the reaction for the oxidative dissolution of AuNPs to $AuBr_4^-$.[49]

$$Au + 4Br^- \rightarrow AuBr_4^- + 3e^- \qquad (10)$$

From the SA/V ratios, the radii (*r*) of the immobilized gold particles deposited at varying times were calculated (Table 2).

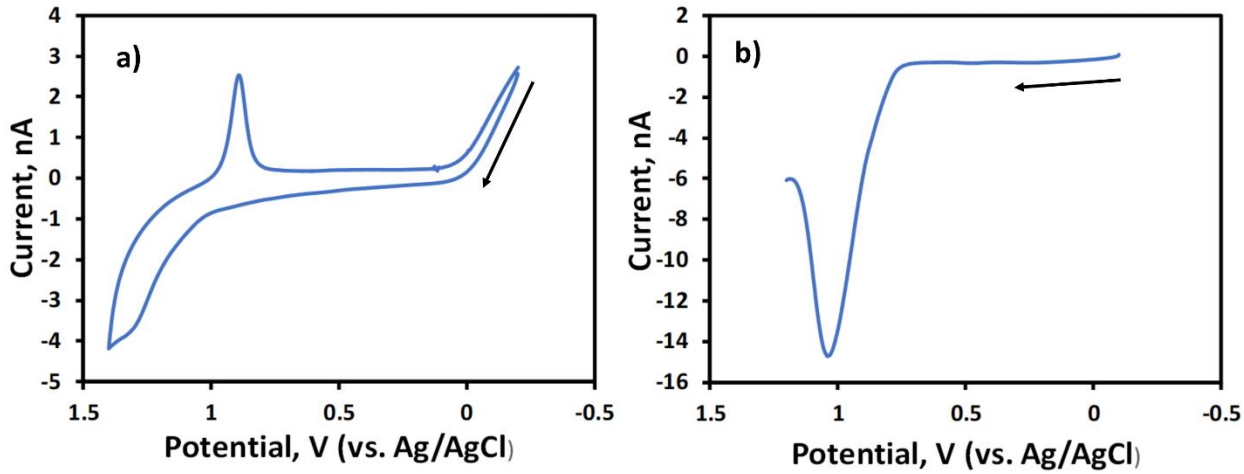


**Figure 5:** Electrochemical responses of immobilized AuNPs on N-CF-UME for NP size determination. a) CV response obtained in 0.1M $HClO_4$ showing Au oxide reduction peak (884 mV) for SA determination. b) Linear sweep voltammetric response in 0.01M KBr (containing 0.1M KClO4) showing the $AuBr_4^-$ peak (1030 mV) for NP volume determination. Immobilization time was 30 minutes. The scan rates were 100 mV/s and 5 mV/s in $HClO_4$ and KBr solutions respectively.

Since we followed the soft nitriding protocol developed by Liu et al., we expected that gold particles immobilized on our N-CF-UMEs would have sizes comparable to those reported by Liu et al. (1.6 nm to 10 nm diameter) on soft nitrided carbon blacks and mesoporous carbons.[46] However, our results (Table 2) showed that we obtained larger size gold particles (33 nm to 136 nm radius).

**Table 2**: Electrochemically determined radii of immobilized AuNPs based SA to volume ratio showing the effect of immobilization time on AuNP size.

| Electrode Type | Time (min) | Trial | $E_{p,AuBr_4^-}$ (mV) | SA (nC) | V (nC) | SA/V | Avg. SA/V | Avg. *r* (nm) |
|---|---|---|---|---|---|---|---|---|
| **N-CF-UME** | 10 | 1 | 950 | 0.4914 | 5.1831 | 0.095 | 0.090 | 33 |
| | | 2 | 940 | 2.4412 | 28.5906 | 0.085 | | |
| **N-CF-UME** | 30 | 1 | 1030 | 0.7176 | 14.8801 | 0.048 | 0.049 | 61 |
| | | 2 | 980 | 3.6931 | 71.7402 | 0.051 | | |
| **N-CF-UME** | 60 | 1 | 1100 | 2.5350 | 114.5002 | 0.022 | 0.022 | 136 |
| | | 2 | 1050 | 2.9912 | 140.4001 | 0.021 | | |
| **CF-UME** | 720 | 1 | 973 | 0.5034 | 134.5402 | 0.0034 | 0.0034 | 802 |

Larger gold particles observed on our N-CF-UMEs could be due to aggregation. Nanoparticle synthesis involves two stages: nucleation and growth.[57,58] For NPs to form on electrode supports, there must first be an active (nucleation) site on the surface of the electrode on which the atoms of the metal precursor form a nucleus of the NP. Nucleation is subsequently followed by the growth of this nucleus into a crystal (the NP). The size and shape of the synthesized metal particle is influenced by many parameters including the density of nucleation sites, the number and rate of growing nuclei and the dimensions of the zone (space) over which a nucleus grows into the particle of interest (without interference from other growing nuclei).[57,58,59,60,61] Electrodes with larger surface areas contain more nucleation sites and larger zones over which growth can occur. While our group used a single strand of carbon fiber of average surface area $8.2 \times 10^{-8}$ $cm^2$, Printex G carbon black, used as electrode support by Liu et al. offered a much larger surface area (2.9 $cm^2$) for gold immobilization. In the presence of $NaBH_4$, the extremely small surface area of our N-CF-UME means there is little-to-no competition for particle growth at the nitrogen-containing sites, resulting in the formation of larger aggregates.

Besides being inexpensive and fast, sizing of NPs based on the electrochemical SA/V technique has been reported to agree well with measurements based on electron microscopy.[49] However, application of this technique has some limitations. Though electrochemical SA/V requires no knowledge of surface coverage (number of AuNPs on the electrode surface), Sharma et al. found that surface coverage (characterized in terms of charge for the peak related to particle volume) did seem to play a role in sizing accuracy.[49] They observed that at low coverages ($10^{-5}$ C and lower), the calculated SA/V ratios were relatively constant. However, as surface coverage increased ($10^{-4}$ C and above), the calculated SA/V ratios were smaller than the expected values based on nanoparticle size. They explained that, as surface coverage increases, contact between

neighboring particles becomes more likely, resulting in larger aggregates and decreasing the exposed surface area of the particles.

Compared to coverages used by Sharma et al. ($10^{-6}$ C to $10^{-4}$ C), our surface coverages were orders of magnitude smaller in the $10^{-9}$ C region (Table 2). However, their electrode size was different from that used in our studies. While we used N-CF-UMEs ($8.2 \times 10^{-8}$ $cm^2$), indium-tin-oxide (ITO) coated glass electrodes (1.4 $cm^2$) were used by Sharma et al., so it would be unfair to compare coverage directly on the basis of charge. A comparison based on charge density (charge per electrode area) should allow us to compare surface coverage in a way that accounts for the large differences in electrode sizes. Our surface coverage was in the $10^{-2}$ to 1 $C/cm^2$ range, which is orders of magnitude larger than that used in the studies of Sharma et al. ($10^{-6}$ to $10^{-4}$ $C/cm^2$)[49]. Larger surface coverages reported in our studies may have resulted in lower SA/V ratios, and an overestimation of particle size. However, it seems most likely that the deposition process led to overgrowth of AuNPs and immobilization of mostly large aggregates.

Overgrowth and aggregation of AuNPs on N-CF-UMEs is also apparent from LSVs of oxidative dissolution in $KBr/KClO_4$ (Figure 6). NP sizing based on electrochemical SA/V assumes complete oxidative dissolution of every gold atom in all AuNPs present on the electrode to $AuBr_4^-$.[49] Complete oxidative dissolution of the gold particles into solution would mean that, after the initial scan of the gold-modified electrode in the $KBr/KClO_4$ solution, any subsequent scan(s) of the same electrode in a $KBr/KClO_4$ solution should not exhibit any $AuBr_4^-$ peak(s) (Figure 6a). However, our results indicated that $AuBr_4^-$ peaks (Figure 6b) could sometimes be observed even after more than 10 scans with each scan being performed in a fresh $KBr/KClO_4$ solution. Each time, the $AuBr_4^-$ peak occurred at about the same potential as that of the initial

scan. This observation could indicate that the extensive AuNP coverage essentially resulted in a bulk layer of gold which could not be completely converted to $AuBr_4^-$ even after multiple scans.

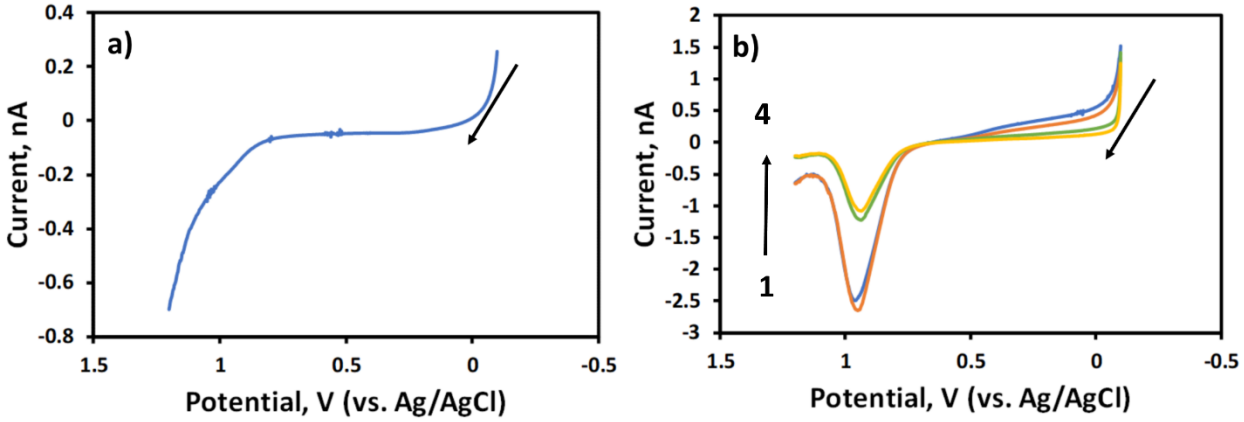


**Figure 6:** LSV responses of a N-CF-UME in 0.01 M KBr solution (containing 0.1 M $KClO_4$). LSV before (a) and after (b) 10 minutes of gold immobilization. The $AuBr_4^-$ peak (~930 mV to 950 mV) was still seen (b) even after scanning the electrode 4 times (each time in a fresh KBr solution). The down pointing arrows show the direction of the initial scan. Top facing arrow shows the order of LSV scans.

The position of the peak associated with the oxidative dissolution of AuNPs has also been linked to particle size through theory and experiments.[49,53,54,55] Plieth's theory postulated that the peak potential of metal NPs during oxidative dissolution would vary inversely with particle size.62 As NP size decreases, its peak potential for oxidative dissolution is expected to shift to a more negative value. From our results (Table 2), the oxidative dissolution peak potentials for the immobilized particles range from 940 mV to 1100 mV vs. Ag/AgCl and are consistent with potentials for large and aggregated particles. For comparison, Ivanova and Zamborini observed peak potentials from 734 mV to 913 mV for 4 nm to 250 nm gold particles.[55] In another study, Allen et al. reported oxidative dissolution potentials for 4-15 nm particles shifted from 698-757 mV to 928-937 mV upon pH-induced aggregation, while the potential for 50 nm particles was not affected by aggregation and remained constant at 943 mV.[53]

Electrocatalysis of Methanol Oxidation Reaction by Immobilized AuNPs

After estimating the size of the immobilized AuNPs, an attempt was made to determine if the particles were catalytic towards methanol oxidation reaction in deoxygenated NaOH solution. CV experiments of N-CF-UMEs in alkaline media taken in the presence and in the absence of 1.0 M MeOH showed no significant observable differences in shape and demonstrated no apparent catalytic activity (Figure 7a). On the other hand, Au-N-CF-UMEs (Figure 7b) displayed behavior consistent with electrocatalytic activity. CV scans in 1.0 M MeOH led to an increase in oxidation current beginning at about -0.13 V and a shift in the oxidation peak from 456 mV, which corresponds to the formation of the gold oxide layer in the absence of MeOH, to a less positive potential at 259 mV.

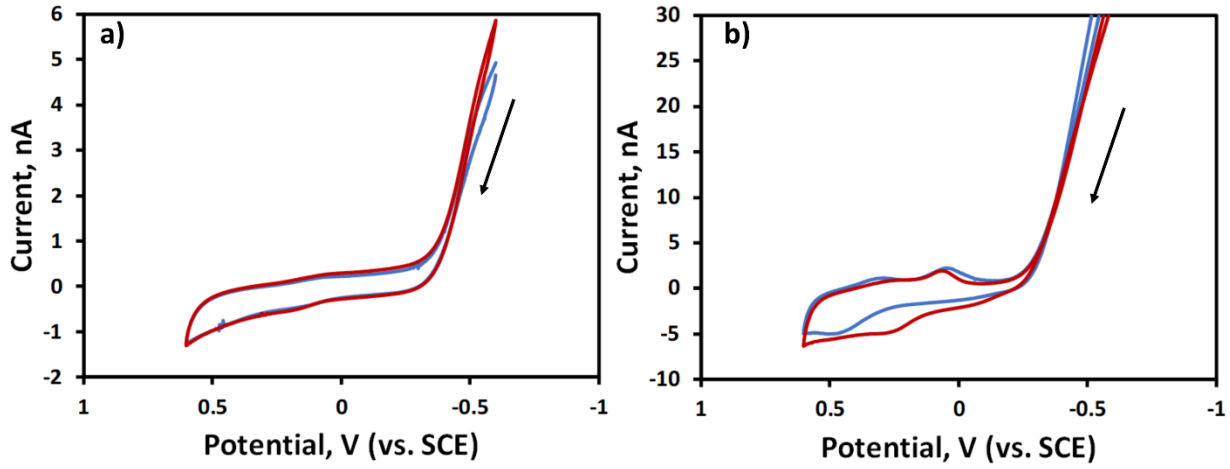


**Figure 7**: CV responses of N-CF-UME in 0.1 M NaOH in the absence and presence of 1.0 M MeOH. N-CF-UME before (a) and after (b) AuNP deposition. Responses in the absence (red line) and presence (blue line) of 1 M MeOH. Immobilization time was 30 minutes. The scan rate was 25 mv/s.

Electrooxidation of organic molecules including alcohols on metal NPs is reported to occur in one of two potential ranges: either in a potential range prior to the formation of surface oxides on the metal (low potential region); or in a potential range where the metal surface is covered with metal oxides (high potential region).[63,64] In the low potential region in alkaline

media, methanol oxidation on gold yields mainly formate (equation 11) while carbonates (equation 12) are mostly produced in the high potential region.[63]

$$CH_3OH + 5OH^- \rightarrow HCOO^- + 4H_2O + 4e^- \quad (11)$$

$$CH_3OH + 8OH^- \rightarrow CO_3^{2-} + 6H_20 + 6e^- \quad (12)$$

Peak potential at 259 mV is in very good agreement with methanol oxidation peak (~254 mV vs. SCE) for 7.2 nm gold NP reported by Yan et al.[63] but is shifted ~160 mV more positive of that reported (~97 mV vs SCE for 0.7- 2.0 nm gold nanoclusters) by Liu et al.[46]

We observed that as methanol concentration was varied, the peak potentials and the peak currents changed (Figure 8). Current continued to increase with increasing methanol concentration upon exposure of the Au-N-CF-UME to methanol at concentrations of 1 to 4 M. However, at 3M methanol, and even though increased current was observed, the peak potential shifted back to a more positive value (401 mV). This suggested a possible decrease in electrocatalytic activity. A positive shift in peak potential with increased methanol concentration continued with maximum current recorded at 4 M methanol (455 mV). At 5 M methanol concentration, peak potential shifted back to a more negative value (381 mV) but with a surprise decrease in current. Overall, these results indicate a loss in catalytic activity upon repeated potential scans and exposure to methanol.

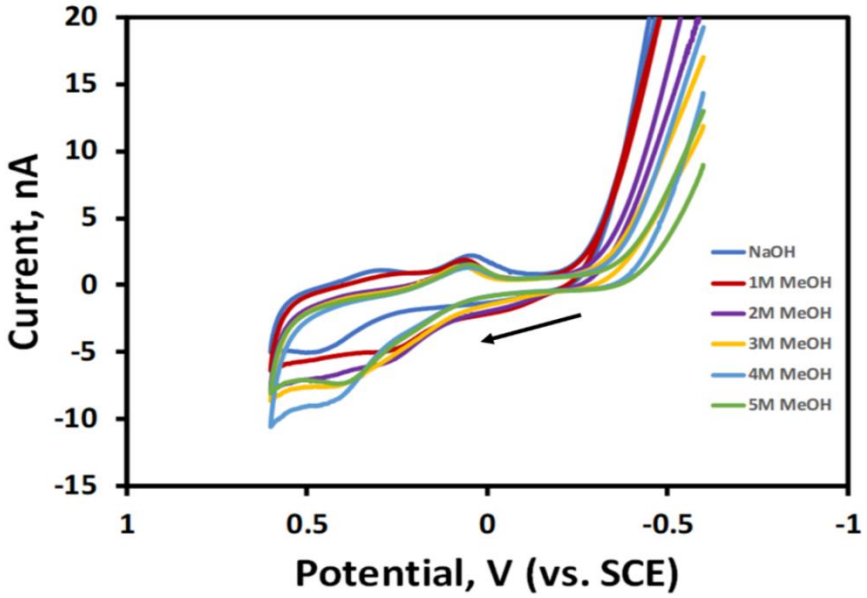


**Figure 8:** CV responses of Au-N-CF-UME in 0.1 M NaOH showing effect of methanol concentration on methanol electrooxidation. Immobilization time was 30 minutes. Scan rate as 25 mV/s.

# CHAPTER 4

# CONCLUSIONS AND FUTURE WORK

## Conclusions

In this study, $NaBH_4$ reduction of $HAuCl_4$ was evaluated as a strategy of immobilizing electrocatalytically active AuNPs on N-CF-UMEs. CF-UMEs and N-CF-UMEs were prepared using a laser-based pipet puller. Electrode sizes were characterized by cyclic voltammetry and found to be 4.52±0.82 μm and 1.62±0.41 μm for CF-UMEs and N-CF-UMEs, respectively. Immobilization of AuNPs was attempted on both N-CF-UMEs and CF-UMEs. Though polyacrylonitrile-based carbon fiber used to prepare CF-UMEs contains some inherent nitrogen species on its surface, doping the carbon fiber with nitrogen was necessary in order to successfully immobilize the AuNPs in a reasonable amount of time. Deposition of AuNPs on N-CF-UMEs could be accomplished in as little as 10 seconds, whereas it took more than 10 hours to get AuNPs on the CF-UMEs.

The effect of deposition time on immobilized AuNP size was determined based on electrochemical SA/V measurements. While the radius of AuNPs adsorbed on the CF-UME after 12 hours was 802 nm, the radii of gold particles immobilized on N-CF-UMEs after 10 to 60 minutes ranged from 33 to 136 nm. However, the particle sizes on N-CF-UMEs were still larger than expected based on a previous report that employed a similar strategy for immobilizing < 2 nm AuNPs on carbon black[46]. Large surface coverages and aggregation due to the much smaller surface area of N-CF-UMEs compared to carbon black are likely responsible for the discrepancy.

Though size measurements indicate mostly large aggregates were deposited on N-CF-UMEs, immobilized AuNPs were still found to be electrocatalytic towards the methanol oxidation reaction. CVs of Au-N-CF-UMEs in the presence of methanol at lower concentration

(1 M) exhibited a peak at 259 mV, which was ~200 mV less positive than Au oxide formation in 0.1 M NaOH. However, exposure of the Au-N-CF-UME to higher methanol concentrations appeared to lead to a decline in catalytic activity as the methanol oxidation peak shifted more positive and current eventually decreased. This may be attributed to the possible inhibition of active sites of the particles by adsorbed intermediates and products of the methanol oxidation reaction[63,64] or restructuring of the Au layer upon repeated oxide formation/reduction cycles.

## Future Work

Following the method used by Liu et al., we expected to get gold particles with diameters between 2 nm and 10 nm. However, our electrochemical calculations based on SA/V showed that our particles are far bigger than expected. A possible reason for this vast discrepancy between our particles and those of Liu et al is an aggregation of the particles. Since our electrode sizes are far smaller than those used by Liu et al., decreasing both gold precursor and reducing agent concentrations might alleviate the aggregation problem. Alternatively, other means of depositing AuNPs such as electrodeposition can be explored to help deposit smaller sized gold particles on N-CF-UMEs. Finally, we hope to translate this kind of deposition method to smaller size carbon fiber electrodes (nanoelectrodes) to enable single NP studies. Even though carbon fiber electrodes (CFEs) are difficult to make smaller, there are reports suggesting ways to make CFEs as small as 1 nm.[34]

REFERENCES


1. Kranz, C.; Mizaikoff, B. Gold Nanoparticles in Analytical Chemistry; 2014; Vol. 66.

2. McKelvey, K.; German, S. R.; Zhang, Y.; White, H. S.; Edwards, M. A. Nanopipettes as a Tool for Single Nanoparticle Electrochemistry. Curr. Opin. Electrochem. 2017, 6 (1), 4–9.

3. Menon, S.; S., R.; S., V. K. A Review on Biogenic Synthesis of Gold Nanoparticles, Characterization, and Its Applications. Resour. Technol. 2017, 3 (4), 516–527.

4. Chan, K. Y.; Ding, J.; Ren, J.; Cheng, S.; Tsang, K. Y. Supported Mixed Metal Nanoparticles as Electrocatalysts in Low Temperature Fuel Cells. J. Mater. Chem. 2004, 505–516.

5. Romero-Romo, M.; Montes de Oca, M. G.; Palomar-Pardavé, M.; Olvera-García, J.; Ramírez-Silva, M. T.; Aldana-González, J. Electrochemical Quantification of the Electro-Active Surface Area of Au Nanoparticles Supported onto an ITO Electrode by Means of Cu Upd. Electrochem. commun. 2015, 56, 70–74.

6. Borkowska, Z.; Tymosiak-Zielinska, A.; Shul, G. Electrooxidation of Methanol on Polycrystalline and Single Crystal Gold Electrodes. Electrochim. Acta 2004, 49 (8), 1209–1220.

7. Iwasita, T. Electrocatalysis of Methanol Oxidation. Electrochim. Acta 2002, 47, 3663-3674

8. Ramli, Z. A. C.; Kamarudin, S. K. Platinum-Based Catalysts on Various Carbon Supports and Conducting Polymers for Direct Methanol Fuel Cell Applications: A Review. Nanoscale Res. Lett. 2018, 13.

9 . Huang, H. X.; Chen, S. X.; Yuan, C. Platinum Nanoparticles Supported on Activated Carbon Fiber as Catalyst for Methanol Oxidation. J. Power Sources 2008, 175 (1), 166–174.

10. Borkowska, Z.; Tymosiak-Zielinska, A.; Nowakowski, R. High Catalytic Activity of Chemically Activated Gold Electrodes towards Electro-Oxidation of Methanol. Electrochim. Acta 2004, 49 (16), 2613–2621.

11. Betowska-Brzezinska, M.; Uczak, T.; Holze, R. Electrocatalytic Oxidation of Mono- and Polyhydric Alcohols on Gold and Platinum. J. Appl. Electrochem. 1997, 27 (46), 13.

12. Yan, S.; Zhang, S.; Zhang, W.; Li, J.; Gao, L.; Yang, Y.; Gao, Y. Application of Carbon Supported $Pt_{core}$-$Au_{shell}$ Nanoparticles in Methanol Electrooxidation. J. Phys. Chem. C 2014, 118 (51).

13. Zhang, D. Electrooxidation of Methanol on Carbon Supported Gold Nanoparticles. Appl. Mech. Mater. 2013, 313–314, 232–236.

14. Bansal, V.; Li, V.; O'Mullane, A. P.; Bhargava, S. K. Shape Dependent Electrocatalytic Behaviour of Silver Nanoparticles. CrystEngComm 2010, 12 (12), 4280–4286.

15. Yu, Y.; Gao, Y.; Hu, K.; Blanchard, P. Y.; Noël, J. M.; Nareshkumar, T.; Phani, K. L.; Friedman, G.; Gogotsi, Y.; Mirkin, M. V. Electrochemistry and Electrocatalysis at Single Gold Nanoparticles Attached to Carbon Nanoelectrodes. ChemElectroChem 2015, 2 (1), 58–63.

16. Shao, M.; Peles, A.; Shoemaker, K. Electrocatalysis on Platinum Nanoparticles: Particle Size Effect on Oxygen Reduction Reaction Activity. Nano Lett. 2011, 11 (9), 3714–3719.

17. Ye, H.; Crooks, R. M. J. Electrocatalytic O2 Reduction at Glassy Carbon Electrodes Modified with Dendrimer-Encapsulated Pt Nanoparticles. Am. Chem. Soc. 2005, 127, 4930–4934 .

18. Kim, D.; Kley, C. S.; Li, Y.; Yang, P. Copper Nanoparticle Ensembles for Selective Electroreduction of CO 2 to C 2 –C 3 Products . Proc. Natl. Acad. Sci. 2017, 114 (40), 10560–10565.

19. Zhou, M.; Kang, Y.; Huang, K.; Shi, Z.; Xie, R.; Yang, W. Ultra-Small Nickel Phosphide Nanoparticles as an High-Performance Electrocatalysis for Hydrogen Evolution Reaction. RSC Adv., 2016, 6, 74895-74902.

20. Chakraborty, S.; Retna Raj, C. Pt Nanoparticle-Based Highly Sensitive Platform for the Enzyme-Free Amperometric Sensing of $H_2O_2$. Biosens. Bioelectron. 2009, 24 (11), 3264–3268.

21. Corradini, P. G.; Pires, F. I.; Paganin, V. A.; Perez, J.; Antolini, E. Effect of the Relationship between Particle Size, Inter-Particle Distance, and Metal Loading of Carbon Supported Fuel Cell Catalysts on Their Catalytic Activity. J. Nanoparticle Res. 2012, 14 (9), No. 1080.

22. Wakerley, D.; Güell, A. G.; Hutton, L. A.; Miller, T. S.; Bard, A. J.; MacPherson, J. V. Boron Doped Diamond Ultramicroelectrodes: A Generic Platform for Sensing Single Nanoparticle Electrocatalytic Collisions. Chem. Commun. 2013, 49 (50), 5657–5659.

23. Zhou, H.; Fan, F. R. F.; Bard, A. J. Observation of Discrete Au Nanoparticle Collisions by Electrocatalytic Amplification Using Pt Ultramicroelectrode Surface Modification. J. Phys. Chem. Lett. 2010, 1 (18), 2671–2674.

24. Xiao, X.; Bard, A. J. Observing Single Nanoparticle Collisions at an Ultramicroelectrode by Electrocatalytic Amplification. J. Am. Chem. Soc. 2007, 129 (31), 9610–9612.

25. Fan, F. R. F.; Bard, A. J. Observing Single Nanoparticle Collisions by Electrogenerated Chemiluminescence Amplification. Nano Lett. 2008, 8 (6), 1746–1749.

26. Zhang, J.; Wei, Y.; Tian, L.; Kang, X. Single Particle Electrochemistry of P-Hydroxythiophenol-Labeled Gold Nanoparticles. RSC Adv. 2015, 5 (61), 49031–49035.

27. Xiao, X.; Pan, S.; Jang, J. S.; Fan, F. R. F.; Bard, A. J. Single Nanoparticle Electrocatalysis: Effect of Monolayers on Particle and Electrode on Electron Transfer. J. Phys. Chem. C 2009, 113 (33), 14978–14982.

28. Chen, S.; Kucernak, A. Electrodeposition of Platinum on Nanometer-Sized Carbon Electrodes. J. Phys. Chem. B 2003, 107 (33), 8392–8402.

29. Oja, S. M.; Fan, Y.; Armstrong, C. M.; Defnet, P.; Zhang, B. Nanoscale Electrochemistry Revisited. Anal. Chem. 2016, 88 (1), 414–430.

30. Li, Y.; Cox, J. T.; Zhang, B. Electrochemical Responses and Electrocatalysis at Single Au Nanoparticles. J. Am. Chem. Soc. 2010, 132 (9), 3047–3054.

31. Ying, Y. L.; Ding, Z.; Zhan, D.; Long, Y. T. Advanced Electroanalytical Chemistry at Nanoelectrodes. Chem. Sci. 2017, 8 (5), 3338–3348.

32. Agyekum, I.; Nimley, C.; Yang, C.; Sun, P. Combination of Scanning Electron Microscopy in the Characterization of a Nanometer-Sized Electrode and Current Fluctuation Observed at a Nanometer-Sized Electrode. J. Phys. Chem. C 2010, 114 (35), 14970–14974.

33. Anderson, T.J.; Zhang, B. Single-Nanoparticle Electrochemistry through Immobilization and Collision. Acc. Chem. Res. 2017, 49 (11), 2625–2631.

34. Chen, S.; Kucernak, A. Fabrication of Carbon Microelectrodes with an effective Radius of 1 Nm. Electrochem. Commun. 2002, 4, 80–85.

35. Penner, R. M.; Heben, M. J.; Longin, T.L.; Lewis, N. S. Fabrication and Use of Nanometer-Sized Electrodes in Electrochemistry. Science. 1990, 250, 1118–1121.

36. Sun, P.; Mirkin, M. V. Electrochemistry of individual molecules in zeptoliter volumes. J. Am. Chem. Soc. 2008, 130, 8241–8250.

37. Branco, P. D.; Mostany, J.; Borrás, C.; Scharifker, B. R. The current transient for nucleation and diffusion-controlled growth of spherical caps. J. Solid State Electrochem. 2009, 13, 565–571.

38. Nogala, W.; Velmurugan, J.; Mirkin, M. V. Atomic Force Microscopy of Electrochemical Nanoelectrodes. Anal. Chem. 2012, 84 (12), 5192–5197.

39. Shao, Y.; Fish, G.; Kokotov, S.; Palanker, D.; Lewis, A.; Mirkin, M. V. Nanometer-Sized Electrochemical Sensors. Anal. Chem. 1997, 69 (8), 1627–1634.

40. Chen, T. K.; Luo, G.; Ewing, A. G. Amperometric Monitoring of Stimulated Catecholamine Release from Rat Pheochromocytoma (PC12) Cells at the Zeptomole Level. Anal. Chem. 1994, 66 (19), 3031–3035.

41. Katemann, B. B.; Schuhmann, W. Fabrication and Characterization of Needle-Type Pt-Disk Nanoelectrodes. Electroanalysis 2002, 14 (1), 22–28.

42. Noël, J. M.; Velmurugan, J.; Gökmeşe, E.; Mirkin, M. V. Fabrication, Characterization, and Chemical Etching of Ag Nanoelectrodes. J. Solid State Electrochem. 2013, 17 (2), 385–389.

43. Fan, Y.; Han, C.; Zhang, B. Recent Advances in the Development and Application of Nanoelectrodes. Analyst 2016, 141 (19), 5474–5487.

44. Sun, P.; Li, F.; Yang, C.; Sun, T.; Kady, I.; Hunt, B.; Zhuang, J. Formation of a Single Gold Nanoparticle on a Nanometer-Sized Electrode and Its Electrochemical Behaviors. J. Phys. Chem. C 2013, 117 (12), 6120–6125.

45. Sun, F.; Gao, J.; Liu, X.; Yang, Y.; Wu, S. Controllable Nitrogen Introduction into Porous Carbon with Porosity Retaining for Investigating Nitrogen Doping Effect on SO2 Adsorption. Chem. Eng. J. 2016, 290, 116–124.

46. Liu, B.; Yao, H.; Song, W.; Jin, L.; Mosa, I. M.; Rusling, J. F.; Suib, S. L.; He, J. Ligand-Free Noble Metal Nanocluster Catalysts on Carbon Supports via “Soft” Nitriding. J. Am. Chem. Soc. 2016, 138 (14), 4718–4721.

47. Affadu-Danful, G. Immobilization of Gold Nanoparticles on Nitrided Carbon Fiber Ultramicroelectrodes by Direct Reduction.MS Thesis, East Tennessee State University, Johnson City, TN, 2018.

48. Deraedt, C.; Salmon, L.; Gatard, S.; Ciganda, R.; Hernandez, R.; Ruiz, J.; Astruc, D. Sodium Borohydride Stabilizes Very Active Gold Nanoparticle Catalysts. Chem. Commun. 2014, 50 (91), 14194–14196.

49. Sharma, J. N.; Pattadar, D. K.; Mainali, B. P.; Zamborini, F. P. Size Determination of Metal Nanoparticles Based on Electrochemically Measured Surface-Area-to-Volume Ratios. Anal. Chem. 2018, 90 (15), 9308–9314.

50. Steven, J. T.; Golovko, V. B.; Johannessen, B.; Marshall, A. T. Electrochemical Stability of Carbon-Supported Gold Nanoparticles in Acidic Electrolyte during Cyclic Voltammetry. Electrochim. Acta 2016, 187, 593–604.

51. Zhang, Y.; Xu, S.; Qian, Y.; Yang, X.; Li, Y. Preparation, Electrochemical Responses and Sensing Application of Gold Disk Nanoelectrodes Down to 5 nm. RSC Adv. 2015, 5, 77248-77254.

52. Adams, K. L.; Jena, B. K.; Percival, S. J.; Zhang, B. Highly Sensitive Detection of Exocytotic Dopamine Release Using a Gold-Nanoparticle-Network Microelectrode. Anal. Chem. 2011, 83 (3), 920–927.

53. Allen, S. L.; Sharma, J. N.; Zamborini, F. P. Aggregation-Dependent Oxidation of Metal Nanoparticles. J. Am. Chem. Soc. 2017, 139 (37), 12895–12898.

54. Masitas, R. A.; Allen, S. L.; Zamborini, F. P. Size-Dependent Electrophoretic Deposition of Catalytic Gold Nanoparticles. J. Am. Chem. Soc. 2016, 138 (47), 15295–15298.

55. Ivanova, O. S.; Zamborini, F. P. Electrochemical Size Discrimination of Gold Nanoparticles Attached to Glass/Indium-Tin-Oxide Electrodes by Oxidation in Bromide-Containing Electrolyte. Anal. Chem. 2010, 82 (13), 5844–5850.

56. Kwon, Y.; Lai, S. C. S.; Rodriguez, P.; Koper, M. T. M. Electrocatalytic Oxidation of Alcohols on Gold in Alkaline Media: Base or Gold Catalysis? J. Am. Chem. Soc. 2011, 133 (18), 6914–6917.

57. Thanh, N. T. K.; Maclean, N.; Mahiddine, S. Mechanisms of Nucleation and Growth of Nanoparticles in Solution. Chem. Rev. 2014, 114 (15), 7610–7630.

58. Velmurugan, J.; Noël, J. M.; Nogala, W.; Mirkin, M. V. Nucleation and Growth of Metal on Nanoelectrodes. Chem. Sci. 2012, 3 (11), 3307–3314.

59. Liu, H.; Penner, R. M. Size-Selective Electrodeposition of Mesoscale Metal Particles in the Uncoupled Limit. J. Phys. Chem. B 2002, 104 (39), 9131–9139.

60. Penner, R. M. ChemInform Abstract: Mesoscopic Metal Particles and Wires by Electrodeposition. ChemInform 2010, 33 (25), no-no.

61. Aliofkhazraei, M. Handbook of Nanoparticles. Handb. Nanoparticles 2015, 1–1426.

62. Plieth, W. J. Electrochemical Properties of Small Metal Clusters. J. Phys. Chem. 1982, 86 (16), 3166–3170.

63. Yan, S.; Zhang, S.; Lin, Y.; Liu, G. Electrocatalytic Performance of Gold Nanoparticles Supported on Activated Carbon for Methanol Oxidation in Alkaline Solution. J. Phys. Chem. C 2011, 115 (14), 6986–6993.

64. Avramov-Ivić, M.; Jovanović, V.; Vlajnić, G.; Popić, J. The Electrocatalytic Properties of the Oxides of Noble Metals in the Electro-Oxidation of Some Organic Molecules. J. Electroanal. Chem. 1997, 423 (1–2), 119–124.

# VITA

## DANIEL KWASI MAWUDOKU

| | |
|---|---|
| Education: | B.S. Chemistry and Biochemistry, University of Ghana, Legon, Accra, Ghana, 2006<br>M.S. Chemistry, East Tennessee State University, Johnson City, TN, 2019 |
| Professional Experience: | Teaching Assistant, University of Ghana; Legon, Accra, Ghana<br>August 2006 – August 2007<br>Teacher, Talent Restoration Academy, Nungua, Accra, Ghana<br>July 2008 – February 2009<br>Sales Executive, Standard Chartered Bank, Accra, Ghana<br>March 2009 – November 2009<br>Marketing Officer, FM Cosmetics and Fragrances Ghana Ltd, Accra, Ghana<br>November 2009 – March 2013<br>Project Coordinator, Volta Lake Fish Farmers' Association, Hohoe, Volta Region, Ghana<br>July 2013 – December 2015<br>Graduate Teaching Assistant, East Tennessee State University, Johnson City, TN<br>2017 – 2019<br>Research Assistant, East Tennessee State University, (Dr. Bishop's Lab)<br>Johnson City, TN<br>2018 – 2019 |
| Research Experience: | Undergraduate Research Student, University of Ghana, Legon, Accra, Ghana<br>2005 – 2006<br>(Supervisor: Dr. W.S.K. Gbewonyo)<br>Extracted fungicide residues from selected pineapple farms and tested their fungicidal activities to cultured fungi species<br>Research Assistant, East Tennessee State University, Johnson City, TN<br>2018 –2019<br>(Supervisor: Dr. Gregory Bishop)<br>Fabricated carbon fiber and CVD carbon electrodes<br>Synthesized bare and capped nanoparticles<br>Immobilized nanoparticles on ultramicroelectrodes for electrochemical studies |
| Community Outreach: | Professional Presenter (Volunteer), National Chemistry Week, |

Toy F. Reid Employee Center, East Chemical Company,
Kingsport, TN
October 23, 2018

Educator (Volunteer), Umoja Festival, Johnson City, TN,
Sep 7 - 8, 2018

Welcome Staff (Volunteer), New Students' Welcome-Table for
Fall 2018, East Tennessee State University, Johnson City, TN
Aug 28, 2018

Community Volunteer, Good Samaritan Ministries, Johnson City, TN
Dec 20, 2017

Presentations:

Daniel Mawudoku, Enoch Amoah, Caitlin Milsap,
George Affadu-Danful, Gregory W. Bishop
Eastman Chemical Company, Kingsport, TN,
October 16, 2018
Nitrogen-Doping of Carbon Fiber Electrodes as a Strategy for
Immobilization and Characterization of Electrocatalytically Active
Gold Nanoparticles.

Daniel Mawudoku, Enoch Amoah, Caitlin Milsap,
George Affadu-Danful, Gregory W. Bishop
South Eastern Regional Meeting of American Chemical Society
(SERMACS), Augusta, GA
November 01, 2018
Nitrogen-Doping of Carbon Fiber Electrodes as a Strategy for
Immobilization and Characterization of Electrocatalytically Active
Gold Nanoparticles.

Daniel Mawudoku, Enoch Amoah,
George Affadu-Danful, Gregory W. Bishop
Graduate Students Research Seminar, Chemistry Department,
East Tennessee State University, Johnson City, TN
March 22, 2019
Immobilization of Electrocatalytically Active Gold Nanoparticles on
Nitrogen-Doped Carbon Fiber Electrodes.

Daniel Mawudoku, Enoch Amoah,
George Affadu-Danful,Gregory W. Bishop
Appalachian Student Research Forum, Johnson City, TN
April 12, 2019
Immobilization of Electrocatalytically Active Gold Nanoparticles on
Nitrogen-Doped Carbon Fiber Electrodes.

Honors and Awards:

Certificate of Achievement Awarded for First Place in
Master's Group 2 Physical and Chemical Sciences Oral Presentation,
Appalachian Student Research Forum, Johnson City, TN
April 12, 2019.